Experimental observation of three-frequency quasiperiodic solution in a ring of unidirectionally coupled oscillators

L. Borkowski,[*] P. Perlikowski,[†] T. Kapitaniak,[‡] and A. Stefanski[§]
Division of Dynamics, Technical University of Lodz, Stefanowskiego 1/15, 90-924 Lodz, Poland
(Received 22 April 2014; revised manuscript received 27 December 2014; published 8 June 2015)

The subject of the experimental research supported with numerical simulations presented in this paper is an analog electrical circuit representing the ring of unidirectionally coupled single-well Duffing oscillators. The research is concentrated on the existence of the stable three-frequency quasiperiodic attractor in this system. It is shown that such solution can be robustly stable in a wide range of parameters of the system under consideration in spite of a parameter mismatch which is unavoidable during experiment.

DOI: 10.1103/PhysRevE.91.062906 PACS number(s): 05.45.Xt, 05.45.Tp, 07.50.Ek

I. INTRODUCTION

The interaction of dynamical systems and networks of coupled oscillators has been a subject of intensive scientific investigation for the last few decades. In general, such structures of linked oscillators have been studied in the context of various types of synchronization between them or transition from regular system behavior to chaos or hyperchaos. Among the possible ways to chaotic motion a transition via a sequence of consecutive Hopf-type bifurcations can be distinguished—the Landau-Hopf transition to the turbulence [1,2]. Later Newhouse, Ruelle, and Takens (NRT) [3,4] formulated the theorem that just after the third successive Hopf bifurcation the three-dimensional (3D) torus decays into a strange chaotic attractor, in effect, of arbitrarily small perturbation—the so-called NRT scenario. Validity of this scenario has been verified in a large family of dynamical systems. On the other hand, other researchers have shown numerical, experimental, and also analytical results which confirm the possibility of the stable 3D torus existence. Grebogi *et al.* performed a numerical experiment which confirmed that smooth nonlinear perturbations do not destroy the stability of the three-frequency quasiperiodicity [5,6], which is important from the physical application point of view. The three-frequency quasiperiodicity has been also detected numerically in continuum systems defined by the Ginzburg-Landau equation [7] and a variety of papers on three coupled oscillators [8–13]. Moreover, even the existence of a stable four-frequency torus has been observed experimentally in a semiconductor system with *pn* junctions [14]. Further progress in theoretical and numerical analysis of this problem has been developed in the last decade of the 20th century and at the turn of the century [15–21]. In this area, works by Feudel *et al.* [15,16] and Anischenko *et al.* [17] have high significance. They explained the existence of the 3D torus as an effect of a certain kind of the system's symmetry and demonstrated possible ways to chaos via three-frequency quasiperiodic solution. Other interesting results in this area of research, particularly in the context of our work, showed the transition to high-dimensional chaos via destruction of the 3D torus in a ring of unidirectionally coupled oscillators [22–24]. Also in recent years some cases of multifrequency quasiperiodic behavior have been reported [25–27]. These works concern self-excited or externally excited oscillators. However, even more interesting are recent reports on chains or globally coupled phase oscillators with frequency detuning which allow us to observe dimensionally growing quasiperiodic regimes, e.g., four- and five-frequency torus [28,29], as in the classical Landau-Hopf scenario.

Especially noteworthy are reports on the experimental detection of quasiperiodic solutions of higher dimension ($\geqslant 3$). Besides the case mentioned above [14] the frequency quasiperiodicity has been observed in an experimental mechanical system composed of a forced elastic cable with concentrated masses [30]. Earlier, the way to chaos via a three-frequency quasiperiodic solution has been demonstrated experimentally in work by Linsay and Cumming [31]. In other cases, the experimental transition from quasiperiodicity to chaos, in which there are still visible traces of a three-frequency torus, i.e., its decay into a strange attractor is not complete, has been observed by Libchaber *et al.* [32] (Rayleigh-Bénard experiment with helium) and Martin *et al.* [33] (power spectrum of the BSN crystal).

In the present work the dynamics of the ring (closed array) of unidirectionally coupled single-well Duffing oscillators is analyzed. Numerical simulations are compared and verified by experiment carried out on a specially constructed electrical circuit. We have concentrated on the existence of the 3D quasiperiodic attractor in this system. The existence of the 3D torus in a ring of three unidirectionally coupled Lorenz systems has been demonstrated and analyzed in detail by Pazo *et al.* [22,23] and Sanchez *et al.* [24]. Unfortunately, they detected numerically this interesting effect only in a very narrow range of control parameters. Therefore it was very difficult to verify this numerical result experimentally, due to the influence of noise or parameter mismatch, which is unavoidable in the real electrical circuit [24]. We show, coming back to these papers, that such 3D torus can be robustly stable in a wide range of parameters of the ring system under consideration, even in the presence of parameter mismatch. According to the above-mentioned concepts, the phenomenon of the three-frequency quasiperiodicity accompanies the transition from regular (periodic) to irregular (chaotic, hyperchaotic) dynamics along the ring. Speaking more precisely—from a so-called *periodic rotating wave* to a *chaotic rotating wave* [22,24].

[*]borek1111100@wp.pl
[†]gimili@p.lodz.pl
[‡]tomaszka@p.lodz.pl
[§]steve@p.lodz.pl

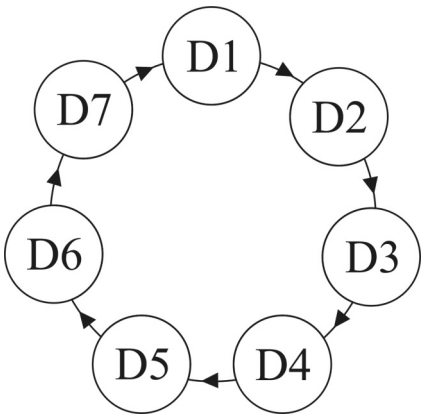

FIG. 1. Scheme representing a ring of seven unidirectionally coupled oscillators.

II. THE SYSTEM

The system under consideration is a closed ring of N unidirectionally coupled oscillators, shown in Fig. 1. As a node system we took an autonomous single-well Duffing oscillator given by

$$\ddot{x}_j + d_j\dot{x}_j + a_j x_j + b_j x_j^3 = 0, \tag{1}$$

where a_j, b_j, and d_j are real positive parameters. Introducing the substitution $y_j = \dot{x}_j$ and assuming diffusive coupling between the oscillators we can describe the dynamics of each jth ring node by the following pair of first-order Ordinary differential equations (ODEs):

$$\begin{aligned} \dot{x}_j &= y_j, \\ \dot{y}_j &= -a_j x_j - b_j x_j^3 - d_j y_j + \sigma(\mu_j x_{j-1} - \kappa_j x_j), \end{aligned} \tag{2}$$

where σ is an overall coupling coefficient, which is considered as the control parameter; μ_j, κ_j are coupling coefficients for each individual oscillator.

III. EXPERIMENTAL CIRCUIT

For the purpose of experimental analysis the real circuit, shown in Fig. 2, has been constructed. This network is composed of seven electrical Duffing oscillators coupled according to unidirectional configuration (see Fig. 1) given by Eq. (2). The constructed board is a double-sided PCB, i.e., some paths are routed on the top layer and the remaining ones on the bottom layer. Detailed structural schemes of a single oscillator in the ring and the structure of coupling resistors are shown in Figs. 3(a) and 3(b), respectively. These components of the circuit are also marked with corresponding rectangular boxes 1 and 2 in Fig. 2.

In order to shorten and simplify further presentation, which is based on the description of the single-node system only, we assumed that resistance and capacity in each jth oscillator are represented by the same symbol, i.e., $R_{nj} = R_n$ and $C_{nj} = C_n$, where n is a number of the resistor or capacitor in the jth oscillator [see Figs. 3(a) and 3(b)].

The electrical Duffing system [Fig. 3(a)] consists of LM358N operational amplifiers, AD663JN multipliers, resistors, capacitors, a 2×10 pin header, jumpers, and a power strip. The LM358N operational amplifier is a dual low-power amplifier. The voltage of the amplifier is 3–32 V and the temperature range 0 °C–70 °C. The AD633JN multiplier is characterized by a very high accuracy—the maximum multiplication error is 2%. Its voltage is from ±8 to ±18 V and the temperature range 0 °C–70 °C. The cubic nonlinearity in the system (2) is realized by means of these multipliers. Nominal values characterizing resistors and capacitors are as follows: $R_1 = R_2 = 1.0\,\mathrm{M\Omega}$, $R_3 = R_5 = R_6 = R_8 = R_9 = 100.0\,\mathrm{k\Omega}$, $R_0 = R_4 = R_7 = R_{10} = 10.0\,\mathrm{k\Omega}$, and $C_1 = C_2 = 10.0$ nF.

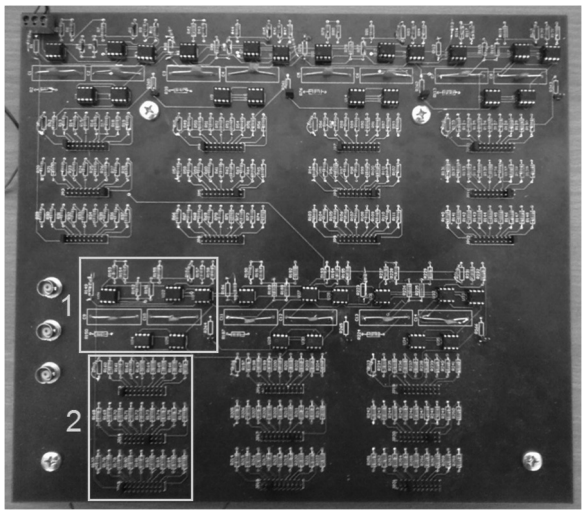

FIG. 2. Electrical circuit of seven unidirectionally coupled, nonlinear Duffing oscillators. One of these subsystems is marked with the rectangular box 1 and the corresponding structure of coupling resistors is marked with box 2.

The Rs resistor, visible in Fig. 3(a), implements a coupling between the oscillators. They are drawn in a simplified manner in Fig. 3(b). In fact, each of the resistors is composed of groups (rows) of resistors, a 2×10 pin header and jumpers by means of which it is possible to set the coupling between adjacent oscillators. Individual resistors connected in rows [Fig. 3(b)] have the following nominal values of resistance: $R_{11} = R_{12} = R_{13} = R_{14} = R_{15} = R_{16} = R_{17} = R_{18} = R_{19} = 10.0\,\mathrm{k\Omega}$, $R_{20} = R_{21} = R_{22} = R_{23} = R_{24} = R_{25} = R_{26} = R_{27} = R_{28} = 1.0\,\mathrm{k\Omega}$, and $R_{29} = R_{30} = R_{31} = R_{32} = R_{33} = R_{34} = R_{35} = R_{36} = R_{37} = 100.0\,\Omega$.

A differential equation of each jth Duffing oscillator, coupled unidirectionally in the ring, was derived on the basis of the circuit scheme shown in Fig. 3(a). A general integral equation illustrating the correlation between the signal components of this circuit is as follows:

$$w_1 = -\frac{1}{R_1C_1}\int w_3 dt - \frac{1}{R_2C_1}\int w_1 dt - \frac{1}{R_3C_1}\int w dt - \frac{1}{R_4C_1}\int w_2 dt. \tag{3}$$

Next, more detailed relationships resulting from the circuit structure [Fig. 3(a)],

$$w = -\frac{1}{R_7C_2}\int\left(-\frac{R_6}{R_5}w_1\right)dt, \quad w_3 = -\frac{R_{s1}}{R_{10}}\left(-\frac{R_9}{R_8}w\right) - \frac{R_{s1}}{R_0}q,$$

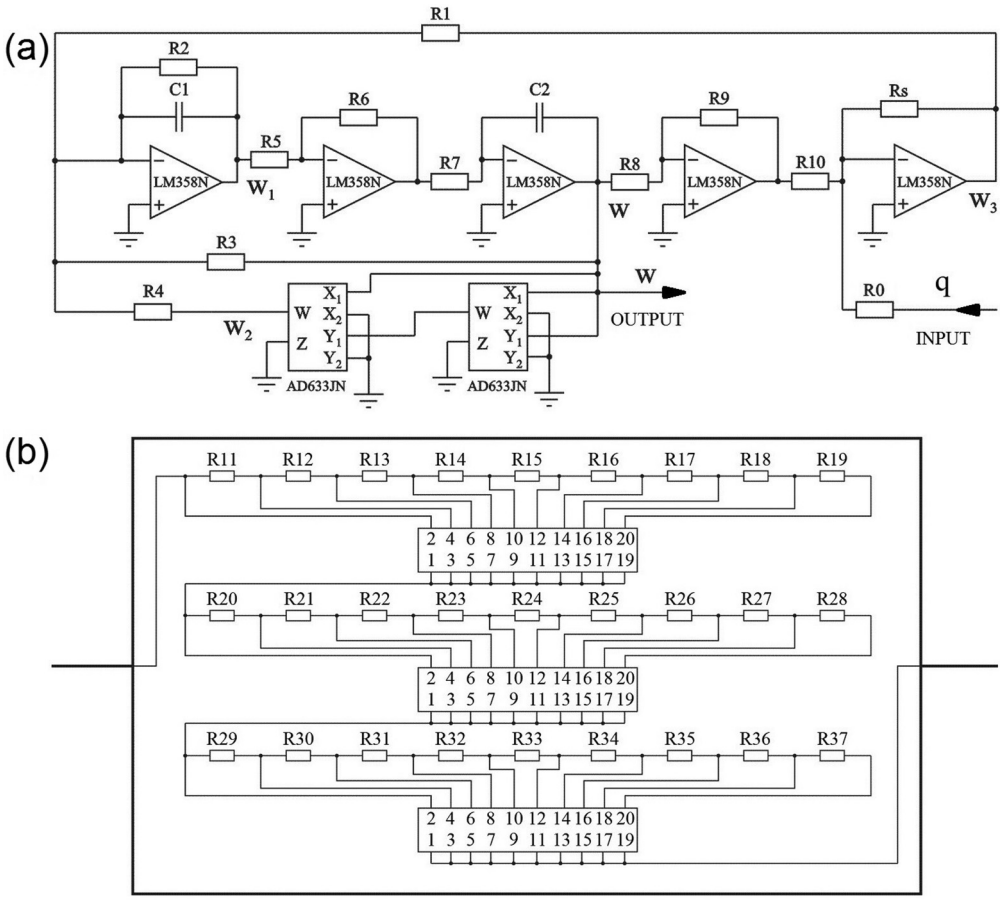

FIG. 3. Schemes of the jth Duffing oscillator coupled in the ring (a) and coupling resistor (b).

and characteristics of the AD633JN multiplier $w_2 = \frac{w^3}{V_M^2}$ can be introduced into Eq. (3). Then, integrating such complemented Eq. (3) we have

$$\ddot{w} + \frac{1}{R_2C_1}\dot{w} + \frac{R_6}{R_3R_5R_7C_1C_2}w + \frac{R_6}{V_M^2R_4R_5R_7C_1C_2}w^3 = \frac{R_6R_s}{R_1R_5R_7R_0C_1C_2}q - \frac{R_6R_9R_s}{R_1R_5R_7R_8R_{10}C_1C_2}w, \quad (4)$$

where $V_M = 10.0$ V is a constant characterizing the AD633JN multiplier and the variable q represents a coupling (driving) signal from the w_{j-1} subsystem. After dividing by $\omega_0^2V_0$ Eq. (4) can be written in a dimensionless form,

$$\frac{1}{V_0\omega_0^2}\ddot{w} + \frac{1}{R_2C_1\omega_0}\frac{1}{V_0\omega_0}\dot{w} + \frac{1}{V_0}w + \frac{R_3}{R_4}\frac{1}{V_M^2V_0}w^3 = \frac{R_3R_s}{R_1R_0}\frac{1}{V_0}q - \frac{R_3R_9R_s}{R_1R_8R_{10}}\frac{1}{V_0}w, \quad (5)$$

where $V_0 = 1.0$ V is a reference voltage (see Ref. [34]) and $\omega_0^2 = \frac{R_6}{R_3R_5R_7C_1C_2}$ represents a nominal frequency of the system (1), i.e., calculated for nominal resistances given above. Hence, the reference value for all subsystems is $\omega_0^2 = 10^7$ s^{-2}, so $\omega_0 = 3162.3\,\mathrm{s}^{-1}$. Finally, Eq. (5) takes the general form of Eq. (2) after taking into account the actual parameter mismatch and the following substitutions introducing dimensionless variables:

$$x_j = \frac{w_j}{V_0}, \quad \dot{x}_j = \frac{\dot{w}_j}{V_0\omega_0}, \quad x_j = \frac{\ddot{w}_j}{V_0\omega_0^2},$$
$$x_j^3 = \frac{w_j^3}{V_M^2V_0}, \quad x_{j-1} = \frac{q_j}{V_0},$$

and parameters $a_j = \frac{\omega_j^2}{\omega_0^2}$ (ω_j^2 is calculated according to the same formula as ω_0^2 but for actual values of resistances), $b_j = \frac{R_{3j}}{R_{4j}}$, $d_j = \frac{1}{R_{2j}C_{1j}\omega_0}$, $\mu_j = \frac{R_{3j}R_{sj}}{R_{1j}R_{0j}}$, and $\kappa_j = \frac{R_{3j}R_{9j}R_{sj}}{R_{1j}R_{8j}R_{10j}}$.

Before the experiment the resistances and capacities of the experimental circuit (Fig. 2) had been precisely measured. On the basis of these values dimensionless parameters of the system (2) were calculated using the above formulas. In Table I dimensionless equivalents of real parameters are presented and compared with corresponding nominal rates. As we can see, deviations from the nominal rate are not larger than 5%.

IV. EXPERIMENT VERSUS NUMERICAL SIMULATIONS

In the first stage of studies presented here we have carried out numerical simulations for identical node systems characterized by nominal values of parameters. Then system (2) is reduced to a ring of identical unidirectionally coupled

TABLE I. Dimensionless equivalents of real parameters of individual Duffing oscillators [Eq. (2)] measured from experimental circuit.

J	a_j	b_j	d_j	κ_j	μ_j
1	1.0000	9.940	0.031 67	0.984	0.987
2	1.0065	10.015	0.031 38	0.992	0.993
3	1.0148	10.107	0.031 21	1.004	1.003
4	0.9948	9.898	0.031 53	0.982	0.982
5	1.0393	10.320	0.032 05	1.023	1.021
6	1.0137	10.056	0.031 83	0.998	0.995
7	0.9953	9.853	0.031 49	0.976	0.976
Nominal	1.0000	10.000	0.031 62	1.0000	1.0000

Duffing oscillators,

$$\dot{x}_j = y_j, \quad \dot{y}_x = ax_j - dy_j + \sigma(x_{j-1} - x_j), \tag{6}$$

where a, b, and d assume nominal rates from Table I.

The increasing number of coupled items was analyzed. This analysis showed that for $N \geqslant 5$ there appears a three-frequency quasiperiodic attractor in the investigated system. In Figs. 4(a) and 4(b) a bifurcation diagram of individual node variable and the corresponding course of the four largest Lyapunov exponents (LEs), calculated for the ring of $N = 7$ oscillators, are presented. In Fig. 4(b) the range of the σ parameter, where the 3D torus occurs, is distinguished with the three largest LEs of zero value in the spectrum (black, gray, and black dashed), i.e., (0, 0, 0, −, −, ...). As we can see this solution appears as an effect of consecutive Hopf-type bifurcations, starting from equilibrium through the limit cycle and two-dimensional (2D) torus. Detailed analytical study of the transition from stable equilibrium to the limit cycle via Hopf bifurcation in the ring of coupled Duffing oscillators [Eq. (6)] is presented in Ref. [35]. The 3D torus dominates in the interval $\sigma \in [0.0433, 0.0478]$. Further

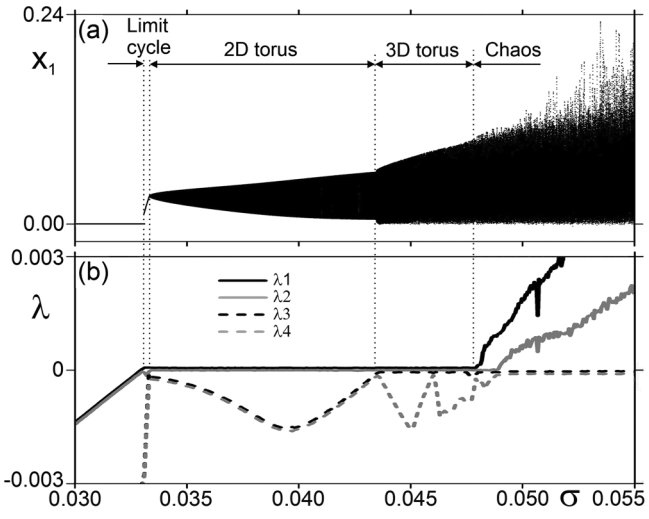

FIG. 4. Bifurcation diagram of individual node variable x_1 (a), and corresponding courses of the four largest LEs (b) for the ring of seven coupled identical Duffing oscillators [Eq. (6)] versus coupling coefficient σ. Parameters: $a = 1.0$; $b = 10.0$, $d = 0.3162$.

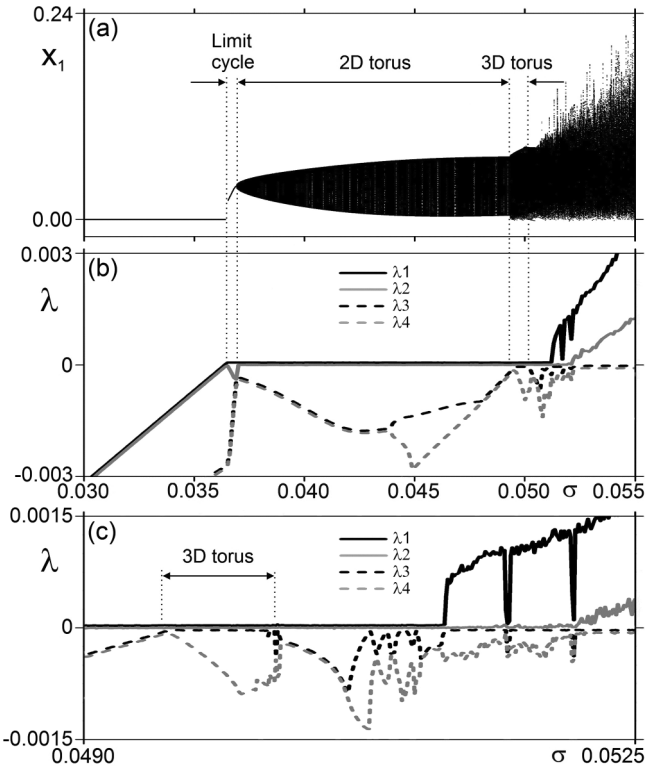

FIG. 5. Bifurcation diagram of individual node variable x_1 (a), corresponding courses of four largest LEs (b) and their enlargement (c) for the ring of seven coupled Duffing oscillators with parameter mismatch [Eq. (2)]. Values of parameters are taken from Table I.

increase of the coupling strength causes destruction of the 3D torus, direct transition to chaos, and next, after a small increase of σ, to hyperchaos on T^2 (2D torus)—two positive and two zero values of LEs (+, +, 0, 0, −, −, ...) in the spectrum.

Being motivated by the above results of numerical simulations, indicating the possibility of 3D torus subsistence in a wide area of the system parameters, we have attempted to confirm these results in the experiment. We decided to build the ring composed of seven oscillators (Fig. 2) because for this case the σ interval of the 3D torus existence achieves relatively large size.

Bifurcation diagrams of the system variable and Lyapunov exponents versus coupling coefficient, computed from a numerical model of a real circuit, are demonstrated in Fig. 5(a), and Figs. 5(b) and 5(c), respectively. As we can see, the inclusion of the parameter mismatch in the numerical model compressed the dimensionless σ range of existence of the 3D quasiperiodic solution. However, the 3D torus still exists, as it is clearly indicated in Fig. 5(b) and its enlargement [Fig. 5(c)] with an interval of three zero LEs ($\sigma \in [0.049\,50, 0.050\,25]$).

The robustness of the three-frequency quasiperiodicity has been proved in experiment. In Figs. 6(a)–6(e) the juxtaposition of numerical and experimental results, which illustrates the transition from periodic [Fig. 6(a)] to chaotic motion [Fig. 6(e)] via 2D torus [Fig. 6(b)], 3D torus [Fig. 6(c)], and torus period doubling [Fig. 6(d)], is presented. Poincaré cross sections [or phase portraits in Fig. 6(a)] and frequency spectra

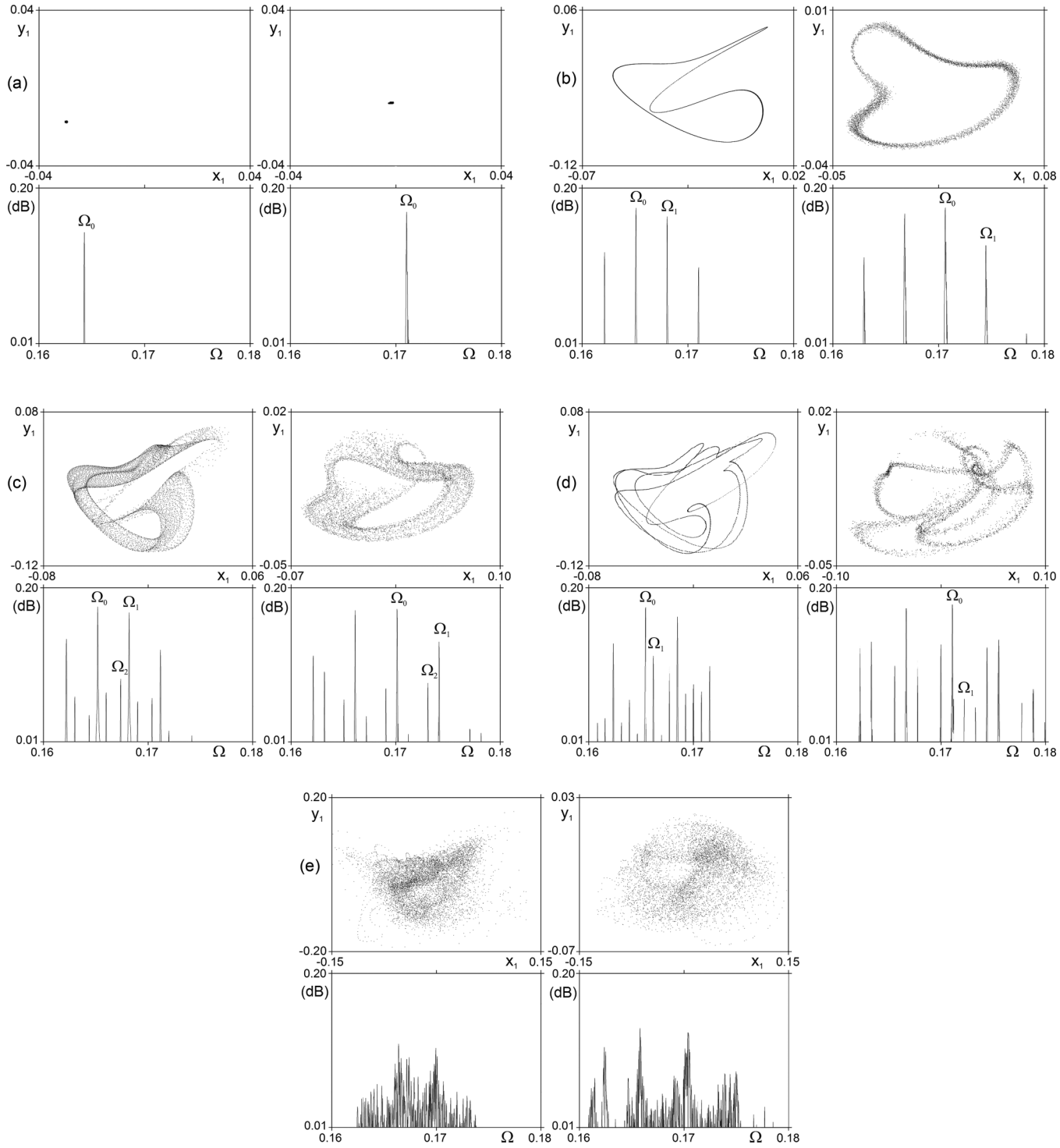

FIG. 6. Juxtaposition of Poincaré cross sections (upper rows) and frequency spectra (bottom rows) simulated numerically—left column: (a) $\sigma = 0.0368$; (b) $\sigma = 0.0490$; (c) $\sigma = 0.0500$; (d) $\sigma = 0.0505$; (e) $\sigma = 0.0515$ and generated experimentally—right column: (a) $\sigma = 0.0490$; (b) $\sigma = 0.0660$; (c) $\sigma = 0.0680$; (d) $\sigma = 0.0700$; (e) $\sigma = 0.0730$.

[fast Fourier transform (FFT) analysis] reconstructed from experiment [right column of Figs. 6(a)–6(e)] are compared with corresponding numerical equivalents [left column of Figs. 6(a)–6(e)]. After a short interval of limit cycle existence [Figs. 2(a) and 2(b)] a wide range of 2D torus continuation occurs with frequency spectra containing two dominant peaks representing incommensurate frequencies Ω_0 and Ω_1 [Fig. 6(b)]. The appearance of a third independent frequency Ω_2 in the spectrum and the structural similarity of Poincaré cross sections reconstructed from experiment and simulations, noticeable in Fig. 6(c), confirm the robust stability of the observed 3D quasiperiodic attractor. Further increase of coupling strength causes the return of 3D torus, next its period doubling [Fig. 6(d)], and after that transition to chaos

on T^2 [Fig. 6(e)], i.e., chaotic motion on 2D torus with the LE spectrum $(+,0,0,-,-,\ldots)$, via a sequence of torus period-doubling bifurcations illustrated by the LE diagram in Fig. 2(c).

We can observe a good agreement of simulations and experiment, although the data collected from the real circuit are disturbed with some noise, which is unavoidable in the experiment. One difference is a shift of experimentally detected solutions to larger values of σ; i.e., bifurcations in the real circuit take place for σ being about 0.012–0.022 bigger than a corresponding numerical one. There is also a visible analogous, but very small shift (about 1%–2%) in frequency spectra [bottom row of Figs. 6(a)–6(e)]. Probably, this problem can be explained by somewhat different saturation limits of individual operational amplifiers in the real circuit. Nevertheless, it is most important here that experimental and numerical sequences of bifurcations and the observed system responses are equivalent.

V. REMARKS AND CONCLUSIONS

Demonstrated results of experimental investigation and its numerical equivalent corroborate that the phenomenon of three-frequency quasiperiodicity can be observed in rings of unidirectionally coupled autonomous Duffing oscillators. Its existence, indicating the qualitative disagreement with the classical NRT scenario [3,4], can be explained by spatiotemporal symmetry of the system under consideration which arises from symmetric Hopf bifurcation appearing due to invariant character of the ring of identical oscillators under the cyclic group [22,36]. It leads to an additional rotational degree of freedom which can be a source of the third incommensurate frequency stabilizing the 3D torus. Then, the ring dynamics can be considered as a superposition of periodic rotational forcing and responses of individual oscillators. Other explanations of this phenomenon are connected with suppression of lockings in modulated rotating waves in systems with rotational symmetry [37] or some disparity in the frequencies of the torus [24]. In the case under consideration high-frequency Ω_0 of the rotating wave coexists with two remaining, incommensurate low frequencies represented by frequency differences Ω_1–Ω_0 and Ω_1–Ω_2 [see frequency spectra in Fig. 6(c)]. Such disparity can diminish an effect of resonant interactions between these frequencies which is destroying for the torus. On the other hand, our study proves that three-frequency quasiperiodicity is kept on, in spite of some symmetry breaking caused by parameter mismatch. However, its relatively considerable influence on the system dynamics [Figs. 5(a)–5(c)] in comparison with the case of identical oscillators [Figs. 4(a) and 4(b)] is clearly visible. This influence manifests with some shift in the sequence of bifurcations in both cases, reducing the range of the 3D torus existence in a disturbed version of the considered ring. In addition, qualitatively different evolution to chaotic motion can be observed. In the case of identical nodes, direct transition from 3D torus to chaos takes place, while for slightly different parameters of nodes return conversion from the 3D to 2D quasiperiodic attractor analysis is observed before the transition to chaos via consecutive torus period-doubling bifurcations.

Summing up, we confirmed numerically and verified experimentally the existence of a stable three-frequency quasiperiodic solution in the ring of unidirectionally coupled Duffing oscillators. The mechanism of such robust stability can be explained as an effect of an additional rotational degree of freedom and its structural separation from the response of oscillators. On the other hand, it has been shown that initiation and propagation of the rotating wave is possible also in rings of real nonidentical oscillators where ideal symmetry of the ring is broken. Moreover, such parameter mismatch does not destroy the three-frequency quasiperiodicity. Our research allows us to conjecture that existence of the three-frequency quasiperiodicity can be a phenomenon which is characteristic for rings of unidirectionally coupled oscillators. Obviously, a verification of this conjecture requires further analysis of such cases which can shed a light on the nature of the rotating wave phenomenon.

ACKNOWLEDGMENT

This work has been supported by the Polish National Centre of Science (NCN) under Project No. UMO-2012/07/N/ST8/03248.

[1] L. D. Landau, Dokl. Akad. Nauk SSSR **44**, 339 (1944).
[2] E. Hopf, Commun. Pure Appl. Math. **1**, 303 (1948).
[3] S. Newhouse, D. Ruelle, and F. Takens, Commun. Math. Phys. **64**, 35 (1978).
[4] D. Ruelle and F. Takens, Commun. Math. Phys. **20**, 167 (1971).
[5] C. Grebogi, E. Ott, and J. A. Yorke, Phys. Rev. Lett. **51**, 339 (1983).
[6] C. Grebogi, E. Ott, and J. Yorke, Phys. D **15**, 354 (1985).
[7] H. T. Moon, P. Huerre, and L. G. Redekopp, Phys. Rev. Lett. **49**, 458, (1982).
[8] C. Baesens, J. Guckenheimer, S. Kim, and R. S. MacKay, Phys. D **49**, 387 (1991).
[9] P. M. Battelino, Phys. Rev. A **38**, 1495 (1988).
[10] P. Ashwin, J. Guasch, and J. M. Phelps, Phys. D **66**, 392 (1993).
[11] P. Ashwin, G. P. King, and J. W. Swift, Nonlinearity **3**, 585 (1990).
[12] P. Ashwin, Chaos, Solitons Fractals **9**, 1279 (1998).
[13] K. Rompala, R. Rand, and H. Howland, Commun. Nonlinear Sci. Numer. Simul. **12**, 794 (2007).
[14] R. Van Buskirk and C. Jeffries, Phys. Rev. A **31**, 3332 (1985).
[15] U. Feudel, W. Jansen, and J. Kurths, Int. J. Bifurcation Chaos Appl. Sci. Eng. **03**, 131 (1993).
[16] U. Feudel, M. Safonova, J. Kurths, and V. Anishchenko, Int. J. Bifurcation Chaos Appl. Sci. Eng. **06**, 1319 (1996).
[17] V. Anishchenko, M. Safonova, U. Feudel, and J. Kurths, Int. J. Bifurcation Chaos Appl. Sci. Eng. **04**, 595 (1994).
[18] J. Yang, Phys. Rev. E **61**, 6521 (2000).
[19] H.-T. Moon, Phys. Rev. Lett. **79**, 403 (1997).

[20] J. M. Lopez and F. Marques, Phys. Rev. Lett. **85**, 972 (2000).
[21] F. Marques, J. M. Lopez, and J. Shen, Phys. D **156**, 81 (2001).
[22] D. Pazo, E. Sánchez, and M. A. Matias, Int. J. Bifurcation Chaos Appl. Sci. Eng. **11**, 2683 (2001).
[23] D. Pazo and M. A. Matias, Europhys. Lett. **72**, 176 (2005).
[24] E. Sánchez, D. Pazo, and M. A. Matías, Chaos **16**, 033122 (2006).
[25] G. V. Osipov, J. Kurths, and S. Zhou, *Synchronization in Oscillatory Networks* (Springer, Berlin, Heidelberg, New York, 2007).
[26] B. Qinsheng, Int. J. Nonlinear Mech. **39**, 33 (2004).
[27] W. Wu, Z. Chen, and Z. Yuan, Chaos, Solitons Fractals **39**, 2340 (2009).
[28] V. Anishchenko and S. Nikolaev, Int. J. Bifurcation Chaos Appl. Sci. Eng. **18**, 2733 (2008).
[29] A. P. Kuznetsov, S. P. Kuznetsov, I. R. Sataev, and L. V. Turukina, Phys. Lett. A **377**, 3291 (2013).
[30] R. Alaggio and G. Rega, Phys. D **137**, 70 (2000).
[31] P. Linsay and A. Cummings, Phys. D **40**, 196 (1989).
[32] A. Libchaber and J. Mauer, in *Proceedings of NATO Advanced Summer Institute on Nonlinear Phenomena*, edited by T. Riste (Plenum, New York, 1982), p. 259.
[33] S. Martin, H. Leber, and W. Martienssen, Phys. Rev. Lett. **53**, 303 (1984).
[34] F. N. H. Robinson, IMA J. Appl. Math. **42**, 177 (1989).
[35] P. Perlikowski, S. Yanchuk, M. Wolfrum, A. Stefanski, P. Mosiolek, and T. Kapitaniak, Chaos **20**, 013111 (2010).
[36] J. J. Collins and I. Stewart, Biol. Cybern. **71**, 95 (1994).
[37] D. Rand, Arch. Ration. Mech. Anal. **79**, 1 (1982).